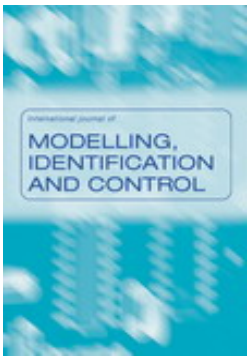

International Journal of Modelling, Identification and Control

ISSN online: 1746-6180 - ISSN print: 1746-6172
https://www.inderscience.com/ijmic

Parameter identification for a model of gas exchange dynamics during cycling

Nadia Rosero, Maxime Chorin, John J. Martinez

DOI: 10.1504/IJMIC.2023.10053834

Article History:

Received:	24 November 2021
Last revised:	04 February 2022
Accepted:	18 February 2022
Published online:	03 February 2023

Parameter identification for a model of gas exchange dynamics during cycling

Nadia Rosero*

Departamento de Electrónica,
Universidad de Nariño,
Pasto, Colombia
Email: nprosero@udenar.edu.co
*Corresponding author

Maxime Chorin and John J. Martinez

GIPSA-Lab,
Grenoble INP,
CNRS,
University of Grenoble Alpes,
38000 Grenoble, France
Email: maxime.chorin@grenoble-inp.fr
Email: john-jairo.martinez-molina@grenoble-inp.fr

Abstract: This paper presents the modelling and parameter identification of the gas exchange dynamics during cycling. A discrete-time linear parameter-varying model is proposed, which relates the dynamics of oxygen consumption and carbon dioxide production with the developed pedal power. A state-dependent nonlinear function is used for modelling the excess carbon dioxide production. The approach proposed for parameter identification is based on specific exercise scenarios tailored to the considered individual, which reduces the data acquisition process. The parameter identification process is performed as a solution of a sequence of nonlinear unconstrained optimisation problems using measured data from different cycling scenarios. An illustration of the methodology used for the identification and the validation of the model is also presented.

Keywords: model identification; gas exchange; cycling; model checking; physiology.

Reference to this paper should be made as follows: Rosero, N., Chorin, M. and Martinez, J.J. (2023) 'Parameter identification for a model of gas exchange dynamics during cycling', *Int. J. Modelling, Identification and Control*, Vol. 42, No. 1, pp.17–30.

Biographical notes: Nadia Rosero received her BSc in Electronics Engineering from the Universidad de Nariño, Colombia, MSc in Automatic Control from the Universidad del Valle, Colombia and PhD in Automatic Control and Production Systems at the University of Grenoble Alpes, France in 2018. She is attached to Universidad de Nariño as a researcher. Her research interests include modelling, control and optimisation applied to renewable energies, production chains and physiological systems.

Maxime Chorin received his BSc in Electrical Engineering and MSc in Automatic Control from the Grenoble Institute of Technology, in 2016 and 2019 respectively. He is currently pursuing his PhD in Automatic Control and Production Systems at the Université Grenoble Alpes, Grenoble, France. His research interest include constrained and robust control, physiological systems and e-bikes.

John J. Martinez received an Electrical Engineering degree and MSc in Automatic Control from the Universidad del Valle, Colombia, in 1997 and 2000, respectively. He received his PhD in Automatic Control from the Institut National Polytechnique de Grenoble, France, in 2005. Presently, he is working as a Full Professor at the Grenoble Institute of Technology, GIPSA-Lab, Control System Department of the University Grenoble Alpes, France. His main research interests include modeling and robust control of mechatronic systems, mostly in: automotive vehicle dynamics, wind turbines control, and physiologic-aware electric bikes.

1 Introduction

A human body performing a cycling workout can be considered as a dynamical system. The whole rider-bicycle system can be seen as an energetic system which transforms chemical energy into mechanical energy. Similar to an electric machine, the mechanical variables as cadence, torque and power allow us to obtain information about the mechanical capabilities of a given human body to produce mechanical effort. On the other hand, physiological variables as gas exchange, heart rate (HR), blood lactate, among others, are often used to determine the physiological capabilities of a cyclist to produce an effort. In this paper, we deal with the modelling and identification of gas exchange dynamics, for a given individual, seen as a consequence of the produced mechanical power during cycling.

Physiology studies provide the basis for understanding the relationships between variables involved in energy transformations within humans (Krogh and Lindhard, 1913; Hill and Lupton, 1923; Casaburi et al., 1989). During a physical activity, molecules of adenosine triphosphate (ATP) are hydrolysed in the muscles in order to ensure the balance between the energy produced and the energy required to perform the exercise. The resynthesis of ATP can occur based on two different pathways: the *aerobic* pathway, in presence of oxygen (O_2), or the *anaerobic* pathway, without oxygen. Thus, to face the increase in energy demand, the human ventilatory system adapts with an increased oxygen consumption, denoted $\dot{V}O_2$ (in l/min) and carbon dioxide production ($\dot{V}CO_2$) to enable ATP resynthesis. Mainly, HR and gas exchange are used to assess human performance during exercise (Abbiss and Laursen, 2005; Noakes, 2000), but gas exchange is considered as a standard method to calculate some widely known physiological indices. The most common is the anaerobic threshold (AT), proposed by Casaburi et al. (1989). The AT marks the onset of a nonlinear increase of $\dot{V}CO_2$ during exercise associated with the metabolic acidosis and is easily identified using the V-slope method during an incremental cycling test (ICT) (Wasserman et al., 1973; Beaver et al., 1986). The AT is used extensively to adapt the intensity of an exercise session to the individual.

The possibility of improving the capacity and performance of human beings in activities such as athletics or cycling, has motivated the research in modelling the relationship between physiological and mechanical variables (Aftalion and Bonnans, 2014; Le et al., 2008; Meyer and Senner, 2018). The interest of obtaining a gas exchange dynamics model for a given individual resides in the capability to estimate and/or predict the behaviour of an individual with respect to the work load.

One approach for the modelling of dynamical systems is the use of physical laws accepted by the scientific community, like energy balances, mass balances or Newton laws. In the case of the respiratory system phenomenological equations based on gaseous pressure or cardiovascular system changes can be used as in Pal et al. (2020). However, there is an inherent difficulty in knowing and measuring the chemical reactions that are occurring within the body. Other popular approaches to model $\dot{V}O_2$ kinetics include models based on a single or multiple exponential functions (Barstow and Molé, 1991; Bell et al., 2001; Casaburi et al., 1989; Hughson et al., 1988). From a control engineering point of view, this behaviour can be modelled by first order differential equations used for describing simple dynamical systems. In Gaskill et al. (2001), other static methods are presented to describe the changes in oxygen consumption or carbon dioxide production. In Olds et al. (1993) and Morton (2006), differential equations are used for the description of oxygen uptake, but calibration of parameters is performed experimentally under strong assumptions. Here, a data-based linear parameter-varying (LPV) dynamical model is obtained for the cyclist gas exchange dynamics, in contrast to phenomenological or static models.

Recently, the control community proposed different approaches to tackle the modelling of gas exchange dynamics. Both Su et al. (2007) and Savkin et al. (2012) proposed to use a nonlinear Hammerstein model to express the transfer between $\dot{V}O_2$ and the running speed, and $\dot{V}O_2$ and the HR and respiratory frequency respectively. Nonlinear models based on machine learning and sensor fusion were proposed in Altini et al. (2015), Beltrame et al. (2017) and Shandhi et al. (2020). Even though the proposed models allow the user to predict the physiological response of the exercising individual their applicability is often restricted to $\dot{V}O_2$ prediction and do not take $\dot{V}CO_2$ into account. Machine learning approaches require the collection of large data bases, which is not always compatible with physiological applications given the fact that data acquisition requires the availability of the considered individual. Also, from a control point of view, nonlinear models are difficult to use in practice in order to design control laws, which could, in this case, enable to adapt or optimise training to the individual (Atkinson et al., 2003).

Our model considers a state-dependent varying parameter in the output which allows the modelling of transitions between two modes:

1 low excess of carbon dioxide (low εCO_2), related with aerobic pathway

2 high excess of carbon dioxide (high εCO_2) related with anaerobic pathway.

This time-varying parameter has been written in terms of a novel physiological index by using a transition function, which significantly helps the classification of those modes. The presented model is intended for conceiving real-time applications as observation, control design and system analysis, as it is illustrated in Rosero et al. (2021) for designing an LPV observer of CO_2. In particular, it is envisaged to use the proposed model to design novel electrical assistance systems for bicycles. Due to the limited size of the available datasets, the proposed structure of the model consist in a limited number of parameters tailored to the individual performing the cycling tests. These

parameters are identified using a sequence of nonlinear unconstrained optimisation problems. The proposed model identification methodology uses different tests according to the varying parameter values as in Huang and Zhao (2018). Results are illustrated and validated by using experimental data of two given individuals in different scenarios.

This paper is an extended version of the work presented in Rosero et al. (2018). The previous work is extended with the explanation of the structure of the gas exchange model, the experiment design, the description of the model identification process with further details, the complete validation process and an illustration of the methodology with experimental data concerning untrained and trained individuals.

Within the context of modelling O_2 and CO_2 dynamics during cycling activities, the direct contribution of the paper is twofold:

1 First, we present a novel dynamical model that simultaneously describes the O_2 and CO_2 dynamics as function of pedal power. In addition, this model also provides information about the excess CO_2 dynamics. This model can be used for simulation, prediction, filtering and/or estimation, both for off-line or on-line applications.

2 Second, we propose a new parameter identification methodology intended for calibration of the model for a given individual. This could be useful for personalised applications. In particular, the parameter identification methodology includes a choice of the model structure intended for reducing the number of parameters to be found. This point is useful for applications where collecting data is difficult or expensive.

The paper is organised as follows: in Section 2, the chemical reactions for producing energy are explained from a physiological point of view. Section 3 reports the procedure, equipment and tests used to obtain the data. Section 4 addresses the proposed approach concerning the system modelling. Section 5 presents the proposed model and its structure. Section 6 describes the parametric identification methodology. Finally, Section 7 illustrates the approach by using measured data of two different individuals on different cycling scenarios and presents the criteria used for the validation of the model.

2 Gas exchange during cycling

The energy required to perform a physical activity is obtained from a series of chemical reactions that transform nutrients into ATP, the muscular energy currency.

According to McArdle et al. (2006), there are mainly three pathways to synthesise ATP:

1 aerobic

2 alactic anaerobic

3 lactic anaerobic.

The aerobic pathway is the most efficient, but requires an adequate supply of oxygen to the muscles and it activates slowly. During the transient required to adapt the respiratory system, energy is produced through the alactic anaerobic pathway. This pathway uses molecules of phosphocreatine (PCr) and adenosine diphosphate (ADP) to synthesise ATP. During moderate and prolonged exercise, energy comes mainly from the aerobic pathway, using firstly glycogen stored in active muscles and liver glycogen, which provides almost half the energy requirement, with the remainder from fat breakdown with minimal amounts from blood glucose.

Examples of aerobic ATP synthesis from glucose and fat can be represented by the reactions (1) and (2), respectively.

$$C_6H_{12}O_6 + 36Pi + 36ADP + 6O_2 \longrightarrow 6CO_2 + 6H_2O + 36ATP \quad (1)$$

$$CH_3(CH_2)_{14}COOH + 130Pi + 130ADP + 23O_2 \longrightarrow 16CO_2 + 16H_2O + 130ATP \quad (2)$$

The above chemical reactions come from the decomposition of substrates to produce ATP and carbon dioxide in presence of oxygen. It is possible to simplify the aerobic ATP synthesis in a very general way as follows:

$$Substrate + O_2 \longrightarrow CO_2 + ATP + \Omega \quad (3)$$

where Ω represents other chemical substances produced during the reaction (including water), and where only the involved molecules are mentioned without specifying their number.

Figure 1 The model for lactic acid buffering by bicarbonate and the control of hyperventilation above ventilatory threshold: from Wasserman et al. (2005) redrawn by Péronnet and Aguilaniu (2006)

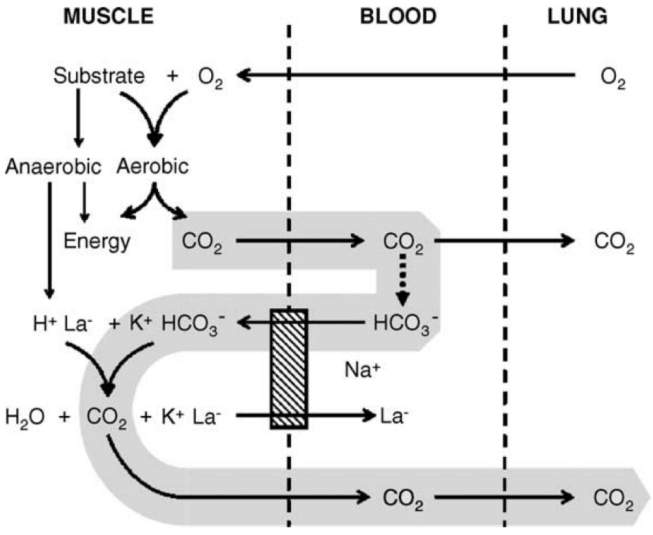

Figure 1 shows a scheme of how energy is obtained from substrates. When a moderate exercise is performed,

energy is mainly obtained through aerobic reactions as equation (3) and carbon dioxide output is proportional to oxygen consumption.

Figure 2 Example of evolution of pedal power, the proposed index $z(k)$, RER and HR during high-intensity and moderate workouts (see online version for colours)

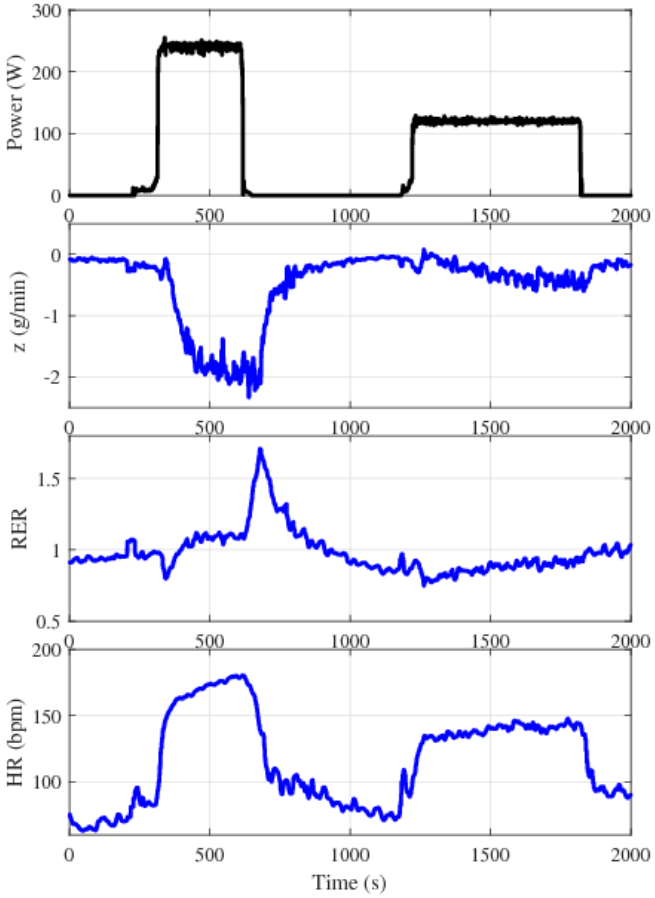

When a supra-maximal exercise is performed, anaerobic reactions occur, where the substrate forms molecules of pyruvate which is then reduced to lactate (La).

$$Substrate \longrightarrow Pyruvates \longrightarrow La + ATP \tag{4}$$

The presence of lactate and an excess of hydrogen ions H^+ activates the lactate clearance mechanisms to maintain proper acid base balance (McArdle et al., 2006). The sodium bicarbonate $NaHCO_3$ in the blood buffers or 'neutralises' the lactate generated during anaerobic metabolism in the following reaction:

$$HLa + NaHCO_3 \longrightarrow NaLa + H_2CO_3 \longrightarrow CO_2 + H_2O \tag{5}$$

In pulmonary capillaries, carbonic acid breaks down into carbon dioxide and water to allow carbon dioxide to readily exit through the lungs. Therefore, that buffering adds 'extra' CO_2 to expired air above the quantity normally released during cellular energy metabolism. Relatively low CO_2 production occurs after exhaustive exercise when carbon dioxide remains in body fluids to replenish bicarbonate that buffered the accumulating lactate. Then, anaerobic pathway implies additional carbon dioxide production. More explanations on the topic of CO_2 overproduction can be found in Wasserman et al. (1973), Wasserman et al. (2005) and Péronnet and Aguilaniu (2006).

It is possible to simplify the anaerobic ATP synthesis in a very general way using equations (4) and (5) as follows:

$$Substrate \longrightarrow CO_2 + ATP + \Omega \tag{6}$$

Equations (3) and (6) do not contain the details of chemical reactions, but they give an idea of the inputs and outputs involved in gas exchange during physical exercise. In this sense, measured variables $\dot{V}O_2$ and $\dot{V}CO_2$ give relevant information about the amount of energy being processed in the body.

3 Experiment description

A physiological dynamical model is highly dependent on the subject. Characteristics such as age, training level, health state or sex change values of parameters. For this reason, in this paper we propose a methodology to identify a model that is tailored to the considered individual. The methodology can be reproducible in similar conditions and using equivalent measurements.

Figure 3 An individual performing a cycling test for system identification (see online version for colours)

Ten apparently healthy adults (including male, female, ranges of age from 17 to 55 and different training levels) perform the protocol test. Results of two male subjects with different training level are shown in Section 7. Similar results were found for the other subjects.

Participants were instructed to avoid alcohol, caffeine, and strenuous exercise on each assessment day and heavy meals 2 hours prior to testing. Visits were separated by a minimum of 24 h.

During visit 1, participants performed a low intensity exercise on the cycle ergometer for familiarisation, allowing them to choose a comfortable pedalling cadence. Then, they performed the ICT from which the AT is identified in order to choose the intensity for next tests.

During visit 2, participants completed the constant power aerobic test (CPAT) followed by a resting period. Then, they performed the constant power anaerobic test (CPAnT).

Finally, during visit 3, participants performed the combined aerobic/anaerobic test (CAAT).

The experimental benchmark is located at GIPSA-Lab, Control System Department. Gas exchange data was collected breath-by-breath and then resampled by interpolation with a constant sampling period of 1 sec. Figure 3 shows an individual performing a cycling test.

3.1 Experimental setup

The used experimental setup is formed by:

- A mechanical cyclist trainer, Hammer (CycleOps, Madison, USA), for setting different cycling scenarios. It provides measurements of pedal power and cadence.
- A medical equipment to measure respiratory gases exchanges during exercise, Metalyzer 3b-R3 (Cortex Biophysik, Liepzig, Germany).
- A chest belt with HR sensor Polar H10 (Polar Electro Oy, Kempele, Finland), which transmits HR data via Bluetooth Low Energy.

3.2 Description of the chosen scenarios

Different datasets are needed for the identification and further validation of the model. Four scenarios are chosen to apply the parametric identification method.

3.2.1 Incremental cycling test

It consists in maintaining a specific cadence while the load is increased progressively, i.e., the load is increased 15W per minute. The test is finished when the cyclist is not able to maintain the power output (imposed by the mechanical cyclist trainer).

3.2.2 Constant power aerobic test

It consists in maintaining a low specific power and constant cadence during pedaling for ten min. The exercise intensity is chosen to perform a moderate exercise, below the AT of the considered individual.

3.2.3 Constant power anaerobic test

It consists in maintaining a high specific power and constant cadence during pedaling for five min. The power level is chosen for performing a high intensity workout (twice the power used during the aerobic test), above the AT of the considered individual. The energy required to perform both the CPAT and the CPAnT is the same, only the power varies.

3.2.4 Combined aerobic/anaerobic test

It consists in a scenario which combines several CPATs and CPAnTs. This scenario contains a moderate intensity workout, a high intensity workout and their associated recovery periods. This scenario is used for the calibration of the transition function (15).

4 Gas exchange model approach

The behaviour of oxygen consumption and carbon dioxide production over time reflects intramuscular biochemical events, humoral transport delays and changes in gas stores as stated in Casaburi et al. (1989). These phenomena are characterised as dynamic processes. In view of these aspects, a static description would suffice neither to represent these dynamical responses, nor to determine a specific flipping point, as in the case of the AT. For this reason, the dynamic behaviour of physiological variables is addressed here by the use of differential equation models.

In practice, the measurements of consumed oxygen and produced carbon dioxide as well as the measurement of the pedal power are available at every time-instant. However, it is not possible to explicitly distinguish the origin of the produced carbon dioxide. It can be produced from aerobic pathway and/or from anaerobic pathway. In this paper, we assume that the output of the system is composed of measured variables. In addition, the knowledge of the relationships between variables coming from chemical reactions and briefly summarised in equations (3) and (6), is taken into account in the structure of the model.

Because using physical laws would lead in this case to a high complexity of the model, we choose to define a structure a priori and identify the value of its coefficient using experimental data. Also, to ensure that our model is compatible with the principle of mass conservation, the quantities of O_2 consumed and CO_2 produce are expressed in mass instead of volume as it is usually found in the litterature.

For the parameter identification of the data-based model, we propose to state an optimisation problem to find the optimal parameters that minimises the error between data and model, calculated by the cumulative sum of the norm-2 of the residuals:

$$\mathbf{e}(k) = \mathbf{y}(k) - \mathbf{y}^m(k) \tag{7}$$

for $k = \{1, ..., N\}$, where $\mathbf{y}^m(k)$ denotes the available measured output data at the instant k, while $\mathbf{y}(k)$ concerns

the obtained output signals by using the models (10)–(11) with measured input data $u(k)$.

5 Structure of the gas exchange model

5.1 Novel index for AT identification

The principle of mass conservation states that for any closed system, the mass of the system must remain constant over time, this means that in a chemical reaction, all of the atoms present at the start of the reaction are present at the end of the reaction. Accordingly, we propose the use of masses per unit of time of O_2 and CO_2, instead of volumes as it is usually found into the literature.

In this way, a novel index for identification of the AT is proposed. It is denoted $z(k)$. It concerns the difference between the mass of oxygen consumption and the mass of carbon dioxide production per unit time. It can be written in terms of $\dot{V}CO_2$ and $\dot{V}O_2$, measured at the instant k, as follows:

$$z(k) := \delta_1 \dot{V}O_2(k) - \delta_2 \dot{V}CO_2(k) \tag{8}$$

where $\dot{V}O_2(k)$ and $\dot{V}CO_2(k)$ are the the flows of oxygen and carbon dioxide respectively in l/min and the constants δ_1 and δ_2 correspond to the volumetric mass density in g/l (or equivalently kg/m^3) of O_2 and CO_2, respectively. The values used here are δ_1 = 1.429 g/l and δ_2 = 1.842 g/l.

An example of the behaviour of the index $z(k)$ for a given individual during a cycling test is shown in Figure 2. Remark that the amplitude of the index $z(k)$ is small and around zero for moderate workout, i.e., for pedal power smaller than 100 W, however it takes more negative values for high-intensity workout, i.e., for pedal power near 200 W. For comparison, the curves concerning the so-called respiratory exchange ratio (RER) and the HR have been included in this figure.

The RER is defined as the ratio between the volumes of produced carbon dioxide and consumed oxygen. That is:

$$RER = \frac{\dot{V}CO_2}{\dot{V}O_2}. \tag{9}$$

This index is usually employed as an approximation of the respiratory quotient (RQ) at cellular level and constitutes an indicator of the substrate (carbohydrate or fat), which is being metabolised. If the value of RER is greater than 1, it is associated to high-intensity exercise and it is often used as a criterion for determining the AT, as it is described in Solberg et al. (2005).

Concerning the HR, it is often used for estimating the amount of pedal power developed by the cyclist. However, this variable does not reach the same values for the same pedal powers and its steady-state values depend on the duration of the exercise.

In this paper, it is proposed to use the index (8) instead of the RER or the HR values for estimating the AT. One of the motivations for this choice is the fact the index (8) easily allows us to distinguish the level of the exercise (moderate or high-intensity workouts). In addition, compared to RER, the index (8) benefits from a good signal to noise ratio. The latter could be explained by the fact that noises on signals are additive in equation (8) while they are multiplicative in equation (9). The proposed index $z(k)$ is quite similar to that proposed and analysed in Issekutz and Rodahl (1961) for estimation of excess CO_2 production. Next, this index is used to classify the dynamical data into two modes: low carbon dioxide production (low εCO_2) or high carbon dioxide production (high εCO_2), as it is depicted in Figure 5.

Figure 4 Equivalent block diagram of the proposed model

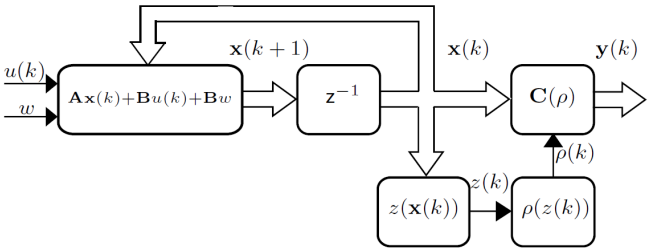

5.2 Structure of the model matrices

An equivalent block diagram of the gas exchange model is depicted in Figure 4. We propose a discrete-time model with input $u(k)$, the pedal power. The output $\mathbf{y}(k)$ is formed by the mass of consumed oxygen y_1 and the mass of produced carbon dioxide y_2, calculated from $\dot{V}O_2$ and $\dot{V}CO_2$ measurements. Assuming that the input and two outputs are available at every constant sample time, the proposed dynamical system follows:

$$\mathbf{x}(k+1) = \mathbf{A}(\theta)\mathbf{x}(k) + \mathbf{B}(\theta)u(k) + \mathbf{B}(\theta)w \tag{10}$$

where the system states at the time instant k are denoted as $\mathbf{x}(k) = \big(x_1(k)\, x_2(k)\, x_3(k)\big)^T \in \mathbb{R}^3$ and its successor $\mathbf{x}(k+1) \in \mathbb{R}^3$. These states concern the mass per unit time of consumed oxygen $x_1 = O_2$, produced carbon dioxide through aerobic pathway $x_2 = CO_2$ and excess of carbon dioxide produced by anaerobic pathway denoted $x_3 = \varepsilon CO_2$. The matrices $\mathbf{A}(\theta) \in \mathbb{R}^{3\times 3}$ and $\mathbf{B}(\theta) \in \mathbb{R}^{3\times 1}$ depend on a vector of constant parameters, denoted θ. These parameters have to be identified for each studied individual. The system inputs are $u(k)$ and w, the pedal power and the basal metabolic rate (BMR), respectively. The BMR w is a physiological quantity characterising the energy consumption of the human body at rest and can be expressed in Watts. It comprises the minimum functions the body requires such as breathing, regulating the body temperature or ensuring the brain activity. In this work we suppose the value of w constant and to be identified along with the other parameters of the model.

The output consists of two variables, one for the total mass per unit time of consumed oxygen, calculated from consumed oxygen and total mass per unit time of produced carbon dioxide, calculated from produced carbon dioxide. That is, $\mathbf{y}(k) \in \mathbb{R}^2$ described as

$$\mathbf{y}(k) = \mathbf{C}(\rho(k))\mathbf{x}(k) \tag{11}$$

where the matrix $\mathbf{C}(\rho(k)) \in \mathbb{R}^{2\times 3}$ is intended to include the different additive contributions on the production of carbon dioxide. The varying parameter $\rho(k)$ allows us to include or exclude the anaerobic contribution of carbon dioxide into the output equation. Thus, the excess carbon dioxide is part of the output whenever a certain number of state conditions hold. Here, it is supposed that the varying parameter $\rho(k)$, which verifies $0 \leq \rho(k) \leq 1$, depends on the system vector $\mathbf{x}(k)$. A hyperbolic tangent function is used for modelling the relationship of $\rho(k)$ with respect to the state vector $\mathbf{x}(k)$.

The system matrices are defined as follows:

$$\mathbf{A} = \begin{bmatrix} \theta_1 & \theta_2 & 0 \\ 0 & \theta_3 & 0 \\ 0 & \theta_5 & \theta_6 \end{bmatrix} \quad \mathbf{B} = \begin{bmatrix} \theta_4 \\ \theta_4 \\ \theta_7 \end{bmatrix} \tag{12}$$

$$\mathbf{C}(\rho(k)) = \begin{bmatrix} 1 & 0 & 0 \\ 0 & 1 & \rho(k) \end{bmatrix} \tag{13}$$

$$0 \leq \rho(k) \leq 1 \tag{14}$$

where θ_i for $i = \{1, ..., 7\}$ are constant parameters depending on the individual. The interest of the proposed matrices structure comes from the fact that we consider that all the system states (mass per unit of time of O_2, CO_2 and εCO_2) are influenced by the pedal power and respond as first order dynamical systems. The latter is justified by the obtained data and by considering that the system involves storage and dissipation phenomena of such gases. Matrices **A** and **B** are shaped according to these assumptions. In addition, in this work it is proposed the inclusion of two more parameters (θ_2 and θ_5 in **A**) for modelling the possible interactions between CO_2 produced in an aerobic way and the values of O_2 and εCO_2. These interactions can be justified from the chemical reactions (3) and (6).

Figure 5 Graphical representation of transition function used to model the progressive transition between two operation modes of the system (see online version for colours)

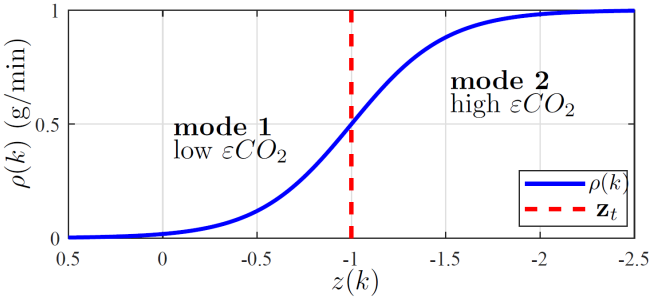

Notes: Here the function follows equation (15) with $\mathbf{z}_t$ = –1 g/min and h = 0.5.

5.3 *Transition function*

The following function is proposed to model the relationship between the parameter $\rho(k)$ and the system states:

$$\rho(k) := \rho(z(k)) = 0.5 + 0.5 \tanh\left(\frac{\mathbf{z}_t - z(k)}{h}\right) \tag{15}$$

where $z(k)$ represents the difference between oxygen consumption and carbon dioxide production at the instant k, as it is defined in equation (8). The symbols $\mathbf{z}_t$ and h are constant parameters that can be identified from experimental data. The choice of function (15) is motivated by the fact that it can be used for modelling abrupt or smooth transitions of $\rho(k)$ around z_t by means of the constant parameter h. The values of $\rho(k)$ are taken between 0 and 1 since it represents the fraction of the excess of carbon dioxide, εCO_2, that can be measured in the ouput of the system.

Figure 6 Scenario for parameter identification of the mode 1: low εCO_2, by fixing $\rho(k)$ = 0, (a) individual 1 (untrained) (b) individual 2 (trained) (see online version for colours)

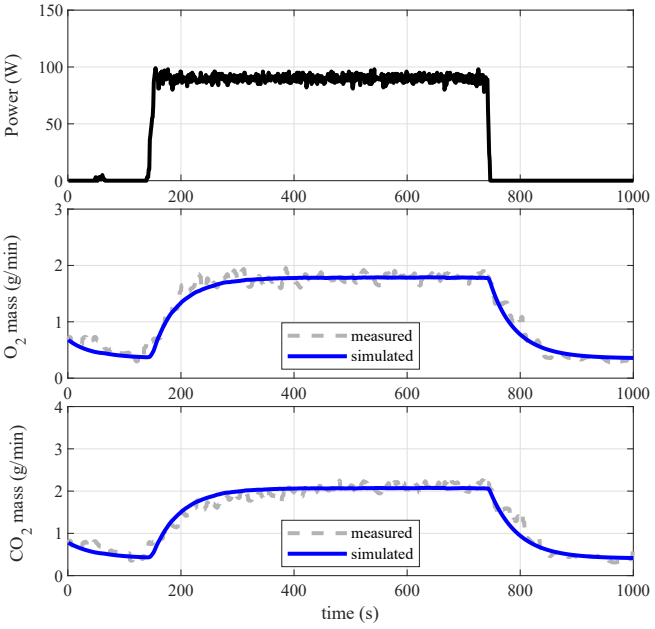

(a)

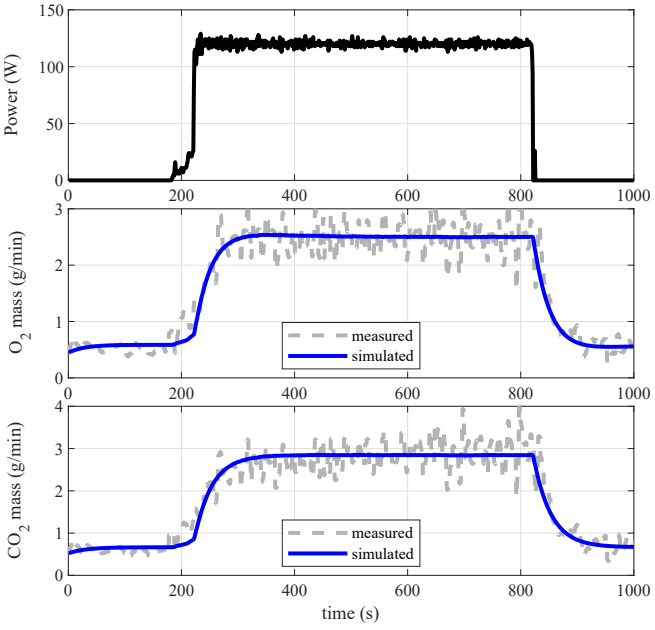

(b)

Thus, here, it is assumed that there is a progressive transition of the observed εCO_2 on the total measured CO_2. Hence, the value of $\mathbf{z}_t$ is the translation of the AT in the $\mathbf{z}$ space, which allow us to define two operation modes, as depicted in Figure 5. They are:

$$\begin{array}{ll} z(k) \leq \mathbf{z}_t & \text{for } \textbf{mode 1}\text{: low } \varepsilon CO_2 \\ z(k) > \mathbf{z}_t & \text{for } \textbf{mode 2}\text{: high } \varepsilon CO_2 \end{array} \tag{16}$$

Thus, the parameter $\rho(k) := \rho(z(k))$ is the percentage of the excess of CO_2, i.e., εCO_2, contained into the total measured CO_2.

6 Parameter identification process

As described in Sename et al. (2013), two main approaches are available to identify LPV systems.

The first one is the *local approach*. It supposes that the varying parameter of the LPV model is available and can be set at *frozen* values while collecting the input and output data necessary to identify linear time invariant (LTI) models around these points by prediction error minimisation. These models are then interpolated to obtain the full model in LPV form.

The second one is the *global approach*. These methods use input and output data as well as varying parameter data, which are directly measured or estimated, in order to identify the model in LPV form. However, these methods require a persisting excitation of the varying parameter during data collection, which can be difficult to ensure in practice.

In the context of this work, the varying parameter is the fraction ρ of εCO_2 that is measured in the output of the system, and can not be directly measured or controlled. This parameter takes continuous values between two extreme setups, the first one being the aerobic state, during low physical effort, and the second one being the anaerobic state, during high physical effort. Based on insights coming from the exercise physiology literature, we proposed equations (8) and (15) to model its behaviour. In this context, neither the *local* or the *global approach* can grasp the problem completely, we thus propose a hybrid approach in the following.

6.1 Optimisation-based parameter identification

The proposed methodology supposes the availability of uniformly sampled data of developed pedal power, flow of consumed oxygen $\dot{V}O_2$ and produced carbon dioxide $\dot{V}CO_2$. Next, the proposed model structure is used to find a vector of parameters $\mathbf{p}$ minimising the simulation error. The identification problem is formulated as:

Find the vector of parameters $\mathbf{p} = [\theta, w, \mathbf{z}_t, h]^T$ which minimises

$$J := \sum_{k=1}^{N} \|\mathbf{y}(k) - \mathbf{y}^m(k)\|_2 \tag{17}$$

subject to

$$\mathbf{x}(k+1) = \mathbf{A}(\theta)\mathbf{x}(k) + \mathbf{B}(\theta)u(k) + \mathbf{B}(\theta)w \tag{18}$$

$$\mathbf{y}(k) = \mathbf{C}(\rho(k))\mathbf{x}(k) \tag{19}$$

$$\rho(k) = \rho(z(k)) \tag{20}$$

for $k = \{1, ..., N\}$, with $u(k)$ the measured input, $\mathbf{y}^m$ the measured output and $\mathbf{y}$ the model output. The function $\rho(z(k))$ defined in equation (15) and $z(k)$ defined in equation (8) and computed using the predicted values from the model.

Due to the nature of the problem and the fact that available data contains different modes, this optimisation problem cannot be solved in one shot. Therefore, a methodology is proposed to solve the problem in three stages using pre-selected sets of data. First, the dynamics of O_2 and CO_2 are identified using data obtained during a moderate intensity cycling session, supposed aerobic. Then, the dynamics of εCO_2 are identified using data obtained during a high intensity cycling session, supposed anaerobic. Finally, the transition function $\rho(z(k))$ defined in equation (15) is identified using data obtained during a training session with both aerobic and anaerobic components.

6.2 Identification of the mode 1: low εCO_2

The parametric identification of the aerobic dynamics requires a sequence of data where the pedal power corresponds to an aerobic exercise, i.e., of moderate intensity. The level of the pedal power for each individual is chosen below the *a priori* AT, calculated with the criterion $RER < 1$.

The identification process is carried out by considering only the parameters describing the aerobic dynamics, they are θ_i for $i = \{1, ..., 4\}$ and w.

Here, $\rho = 0$ because it is assumed that there is no excess of carbon dioxide production in the considered dataset due to the aerobic nature of the effort performed.

The optimisation-based identification problem is formulated as the problem of finding the vector of parameters $[\theta_1, \ \theta_2, \ \theta_3, \ \theta_4, \ w]^T$ which minimises equation (17), subject to equations (18) and (19), with matrices $\mathbf{A}(\theta) = \mathbf{A}_1$, $\mathbf{B}(\theta) = \mathbf{B}_1$ and $\mathbf{C}(\rho(k)) = \mathbf{C}_1$, where,

$$\mathbf{A}_1 = \begin{bmatrix} \theta_1 & \theta_2 & 0 \\ 0 & \theta_3 & 0 \\ 0 & * & * \end{bmatrix} \quad \mathbf{B}_1 = \begin{bmatrix} \theta_4 \\ \theta_4 \\ * \end{bmatrix} \quad \mathbf{C}_1 = \begin{bmatrix} 1 & 0 & 0 \\ 0 & 1 & 0 \end{bmatrix} \tag{21}$$

The value of the coefficients denoted by $*$ is identified during the next steps of the identification process.

6.3 Identification of the mode 2: high εCO_2

The parametric identification of the anaerobic dynamics requires a sequence of data where the pedal power corresponds to an anaerobic exercise, i.e., a high intensity workout. The identification process is carried out by

considering only the parameters describing the anaerobic dynamics, they are θ_i for $i = \{5, 6, 7\}$.

Here, $\rho = 1$ because it is assumed that there is an important excess of carbon dioxide production in the considered dataset. Coefficients θ_i for $i = \{1, ..., 4\}$ and w are set to their identified value.

The optimisation-based identification problem is now formulated as finding the vector of parameters $[\theta_5, \theta_6, \theta_7]^T$ which minimises equations (17), subject to equations (18) and (19), with matrices $\mathbf{A}(\theta)$ and $\mathbf{B}(\theta)$ defined in equation (12) and $\mathbf{C}(\rho(k)) = \mathbf{C}_2$ with:

$$\mathbf{C}_2 = \begin{bmatrix} 1\,0\,0 \\ 0\,1\,1 \end{bmatrix} \tag{22}$$

6.4 Identification of the transition function parameters

Concerning the identification of the parameters of the transition function $\rho(z(k))$, given by equation (15), a data sequence including moderate and high intensity exercise has to be used.

The parameter identification problem can be formulated as follows: find the vector of parameters $[\mathbf{z}_t, h]$ which minimise equation (17), subject to equations (18), (19) and (20), with matrices $\mathbf{A}(\theta)$ and $\mathbf{B}(\theta)$ defined in equation (12) and using the previously obtained parameters, i.e., $[\theta, w]^T$. The matrix $\mathbf{C}(\rho(k))$ defined in equation (13) with $\rho(k)$ defined by equation (15).

The different parameter identification problems, presented in Subsections 6.2, 6.3 and 6.4, can be solved as nonlinear unconstrained optimisation problems, by using for instance the quasi-newton method.

Once parameters of the model are obtained, a validation process is performed using a new set of data independent from the identification datasets.

7 Numerical results

This section presents numerical results obtained from the parametric identification process described in Section 6. For comparison, in this paper is shown one model identified using data from an untrained individual and another one using data from a trained individual.

Two healthy young men performed the previously described cycling tests to identify their personal gas exchange dynamical models using the proposed methodology.

In order to calibrate the exercise intensity associated with the constant power tests, a ICT is performed at a freely chosen cadence (40 rpm and 50 rpm for individuals 1 and 2, respectively). Using data from the ICT, the AT can be identified using the criterion $RER > 1$ (Solberg et al., 2005). Here, individual 1 has to perform more than 150 W to reach the mode 2, and individual 2 has to perform more than 200 W to reach it.

Moderate exercises are performed at 60% of the estimated AT and high intensity exercises at 120% of the estimated AT.

Figure 7 Scenario for parameter identification of mode 2: high εCO_2, by fixing $\rho(k) = 1$, for comparison, the expected aerobic dynamics is also depicted in this figure, (a) individual 1 (untrained) (b) individual 2 (trained) (see online version for colours)

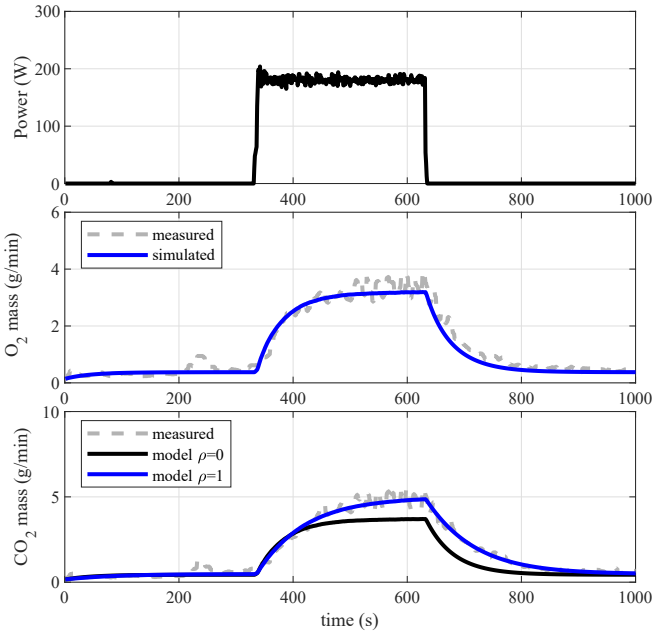

(a)

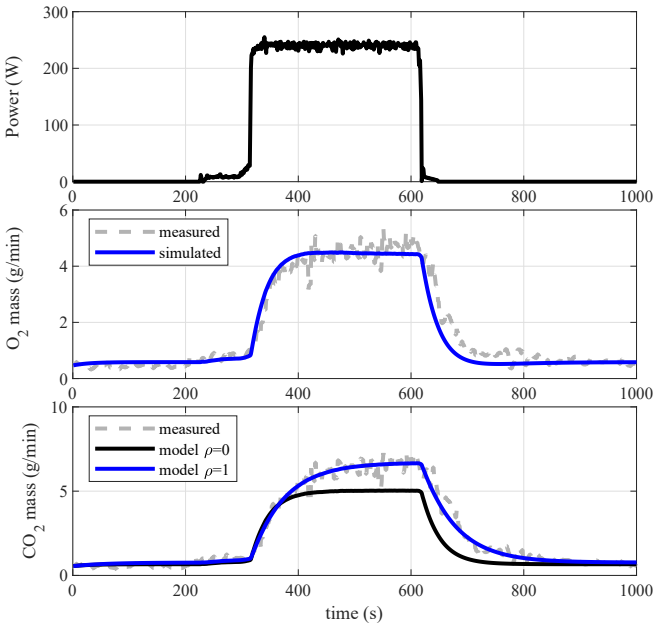

(b)

The identification of the aerobic dynamics or mode 1 is performed by using the CPAT. The results are shown in Figure 6. For both individuals, the model output fits the experimental data of oxygen consumption and carbon dioxide production.

Then, the anaerobic dynamics or mode 2 is identified using data from the CPAnT, for an intense exercise dataset as described in Section 6.3. The results of the identification are shown in Figure 7. Remark that the aerobic dynamics, by considering $\rho = 0$, is not enough to reproduce the carbon dioxide production dynamics. However, in this scenario,

for $\rho = 1$, the obtained model reproduces well the excess of carbon dioxide production. Then, the transition function parameters $\mathbf{z}_t$ and h are identified using data from both the CPAT and the CPAnT.

Figure 8 Model validation for individual 2, by using experimental data from ICT, (a) individual 1 (untrained) (b) individual 2 (trained) (see online version for colours)

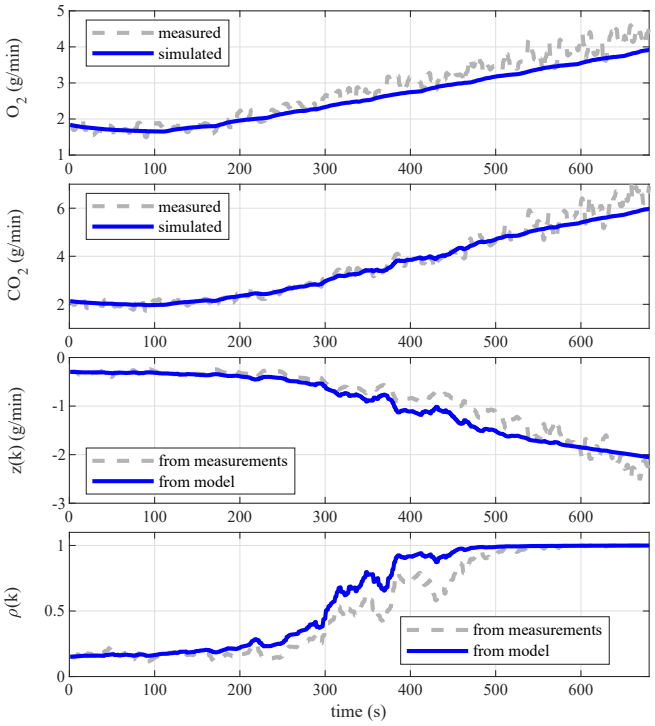

(a)

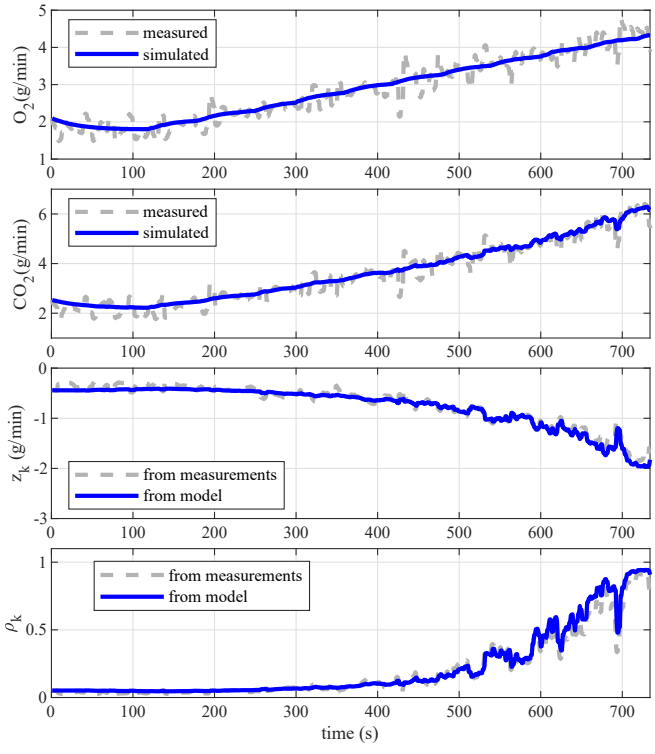

(b)

Figure 9 Residuals calculated for ICT data, bounds are two standard deviations, (a) individual 1 (untrained) (b) individual 2 (trained) (see online version for colours)

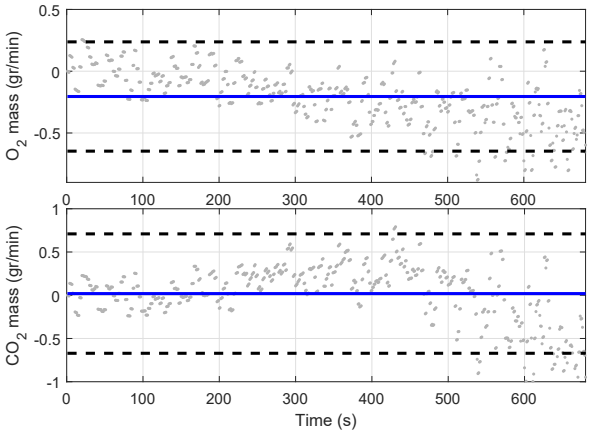

(a)

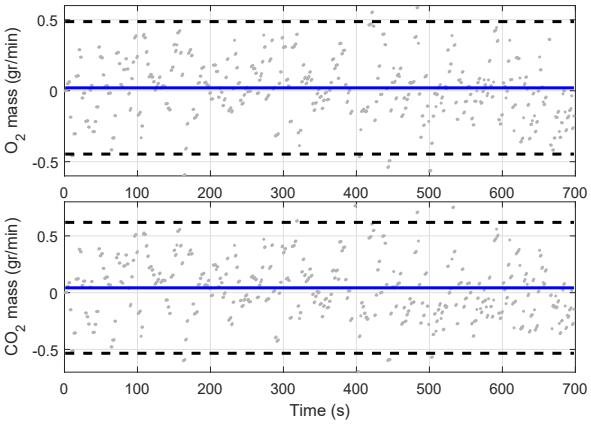

(b)

The identified model for the individual 1 (untrained) is:

$$\mathbf{A} = \begin{bmatrix} 0.943 & 0.029 & 0 \\ 0 & 0.981 & 0 \\ 0 & 0.009 & 0.994 \end{bmatrix} \quad \mathbf{B} = \begin{bmatrix} 0.363 \\ 0.363 \\ 0.029 \end{bmatrix} \times 10^{-3} \tag{23}$$

and the parameters $w = 18.288$, $\mathbf{z}_t = -0.692$ and $h = 0.487$. The identified model for the individual 2 (trained) is:

$$\mathbf{A} = \begin{bmatrix} 0.986 & -0.015 & 0 \\ 0 & 0.973 & 0 \\ 0 & 0.012 & 0.981 \end{bmatrix} \quad \mathbf{B} = \begin{bmatrix} 0.523 \\ 0.523 \\ -0.139 \end{bmatrix} \times 10^{-3} \tag{24}$$

and the parameters $w = 32.03$, $\mathbf{z}_t = -1.218$ and $h = 0.532$.

7.1 Model validation

The dataset used for the validation process should include aerobic and anaerobic sequences of exercises. Here, we use the sequence of data from the ICT, which is not used for identification and meet the requirements of having aerobic and anaerobic exercise. For this work, the model validation is done by using the following validation tests:

Figure 10 Autocorrelation of residuals, (a) individual 1 (untrained) (b) individual 2 (trained) (see online version for colours)

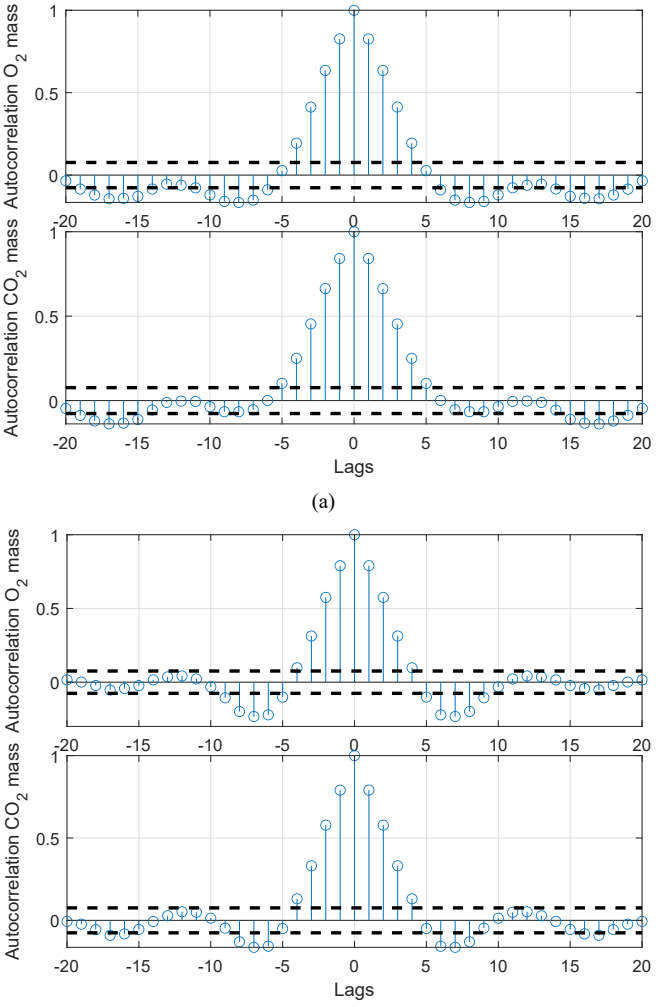

Figure 11 Partial autocorrelation function (PAF) of residuals calculated from validation dataset to assess the order of the model (see online version for colours)

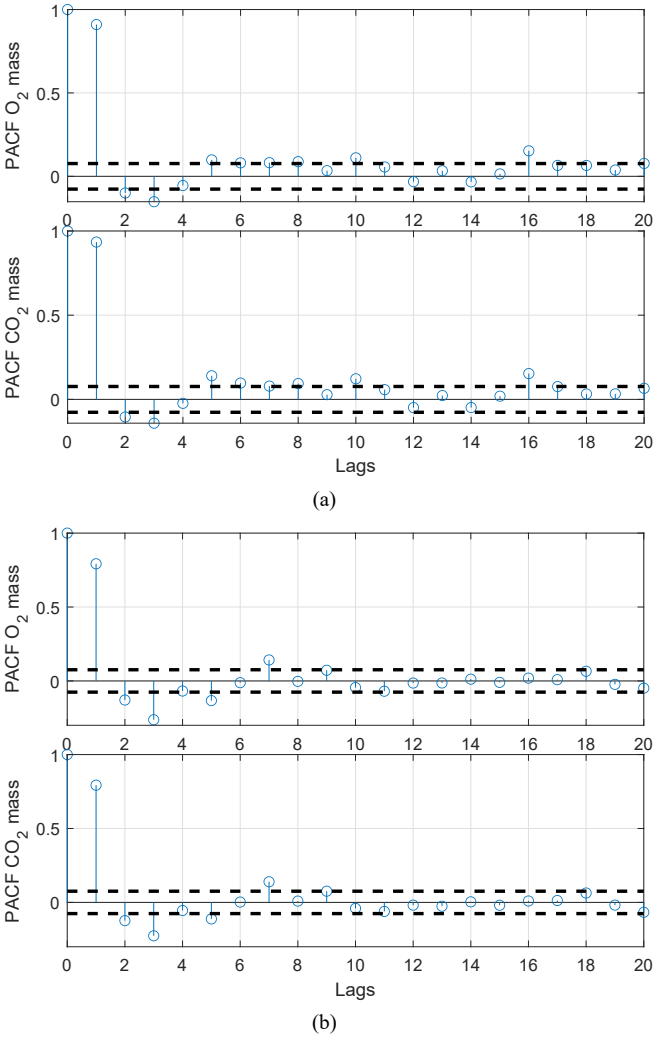

7.1.1 *Residual analysis*

The residuals are formed by simulation error described in equation (7), for N uniform-sampled data.

Table 1 Prediction-error variance of gas exchange models for both individuals for different experimental scenarios

Scenario	*Predicted output*	*Individual 1 variance*	*Individual 2 variance*
CPAT	y_1	0.012	0.060
	y_2	0.020	0.089
CPAnT	y_1	0.041	0.123
	y_2	0.052	0.096
CAAT	y_1	0.021	0.074
	y_2	0.031	0.084
ICT	y_1	0.039	0.051
	y_2	0.068	0.066

Notes: y_1 and y_2 are the mass per unit time of O_2 and CO_2, respectively.

The plots of the residuals are analysed to verify that their behaviour is random and their variance sufficiently small compared to the range of the variable. For the numerical example, the values of variances for each test are shown in Table 1.

The residual plot is shown in Figure 9. For the two cases of individuals the behaviour of the residuals appears to be random and is characterised by an average very close to zero and a low variance compared to the range of the variable. For the case of the oxygen mass residuals for individual 1, the average is near to –0.2 and a slight negative trend is shown, it is also evident in O_2 plot of Figure 8(a). It could suggest a variation in the model from identification scenarios and validation one.

7.1.2 *Goodness of fit*

The goodness of fit or fit-criterion is used for evaluating the accuracy of the model according the normalised root mean square error (NRMSE). The percentage of fit for each sequence of data is determined as:

$$FIT = 100\left(1 - \frac{\|y^m - y\|}{\|y^m - \bar{y}\|}\right) \quad (25)$$

where y^m represents the measured data, y the model output and $\bar{y}$ the mean value of y^m.

For the numerical examples the values of goodness of fit are shown in Table 2.

Table 2 Fit calculated for each stage of identification process

	Individual 1	*Individual 2*
Aerobic dynamics	75%	80%
Anaerobic identification	83%	82%
Validation	74%	81%

The model output and the used experimental data are shown in Figure 8. Remark that the obtained model fitting deviation is small and that the presented curves allow an easy estimation of the ATs (see for instance, the developed power and/or the HR at $\rho(k) = 0.5$).

Table 1 presents the obtained variance for the residuals concerning the system outputs for different scenarios. Remark that these variances are relatively small compared to the minimum and maximum values of such system outputs.

Figure 12 The output space divided by the line $z(k) = \mathbf{z}_t$ (dashed line), which indicates the transition between mode 1 (low εCO_2) and mode 2 (high εCO_2), (a) individual 1 (b) individual 2 (see online version for colours)

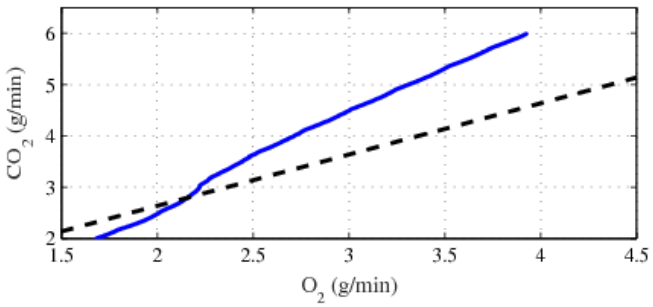

(a)

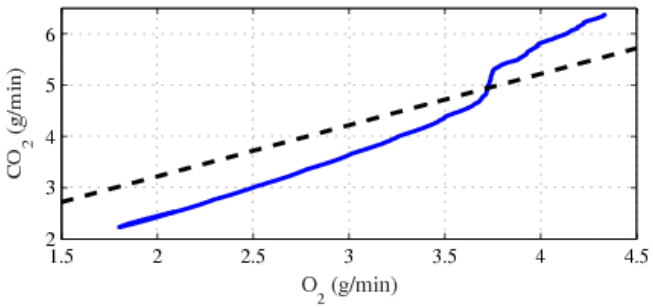

(b)

Note: Solid lines corresponds to the measured data.

7.1.3 *Autocorrelation analysis*

The analysis of autocorrelation measures the strength of association between a signal and a delayed copy of itself. Figure 10 shows the autocorrelation of O_2 and CO_2 residuals for both individuals.

The values of the bounds in Figure 10 are calculated as $\pm 2/\sqrt{N}$, where N is the data-length. These bounds correspond to the 95% confidence interval of a white-noise signal: any data point outside of this interval has a low probability (5%) to have been caused by a white noise. The fact that the values are outside the limits for several lags may be due to the existence of a relationship between lags and may suggest the convenience of a higher order model, for this reason the partial autocorrelation is analysed and the principle of parsimony is taken into account to conclude about the appropriate order of the model.

7.1.4 *Partial autocorrelation analysis*

In this case, we are assuming a linear dependence of the variables at each time instant on the previous time, as can be seen in equation (10), then, we use the PACF to analyse the order of the model.

The partial PACF at lag k is the correlation that results after removing the effect of any correlations due to the terms at shorter lags (Box et al., 2015).

On the hypothesis that the process is autoregressive of order 1, for evaluating a model, the estimated partial autocorrelations of order 2 and higher, must be approximately independently and normally distributed with zero mean.

The partial autocorrelations of the residuals are shown in Figure 11. The values obtained for lags higher than 1 are very low, thus, we conclude that first order models are enough to describe the behaviour of the gas exchange dynamics despite the residual correlations shown in Figure 10.

The proposed low order model seems suitable for simulation and prediction of the output behaviour for different kind of scenarios with enough precision.

7.2 *Analysis of the output space mapping*

The output space mapping concerning the ICT scenario is depicted in Figure 12. The space is divided by a dashed line defined by $z(k) = \mathbf{z}_t$. Such line determines whether the data belong to mode 1 (low production of εCO_2) or mode 2 (high production of εCO_2). During the ICT, the pedal power increases linearly with the time, thus, the crossing between the two modes only occurs once. The crossing point, provided by the model, could be considered as an estimation of the AT. The identification of this threshold seems easy for the individual 2, where the transition between two modes is evident. The case is less simple for individual 1, because the crossover between the two modes is smooth. This mode identification method could be used in addition of the the RER based method in order to identify

the crossing of the AT from experimental data. However, in the case of random cycling scenarios, identifying the AT using this method could be more complex since the line $z(k) = \mathbf{z}_t$ could be crossed several times.

From Figure 12, it is possible to confirm that individuals have different levels of training. See for instance, the maximum level of O_2 and the point where the curves cross the dashed line $z(k) = \mathbf{z}_t$. The higher the training level of the cyclist, the higher the crossing point.

8 Conclusions

In this paper a model for gas exchange dynamics during cycling has been proposed. A methodology for parameter identification and validation of this model has also been presented. The identification process is based on several scenarios that include moderate exercises, high-intensity exercises and ICTs.

A time-varying parameter, in the output matrix, models the transition between two possible modes. A mode is related to low levels of produced excess of carbon dioxide, while a second mode is related to high ones.

In addition, this time-varying parameter has been written in terms of a novel physiological index by using a transition function, which significantly helps the classification of those modes.

The experimental results presented in this paper, demonstrate the model validation according to the fit with the data and therefore the model can be used in simulation, prediction and analysis of consumed oxygen and produced carbon dioxide by using pedal power data. Furthermore, the proposed model can be useful for designing new model-based observers and control laws for future electrical assistance systems.

References

Abbiss, C.R. and Laursen, P.B. (2005) 'Models to explain fatigue during prolonged endurance cycling', *Sports Medicine*, Vol. 35, No. 10, pp.865–898.

Aftalion, A. and Bonnans, J.F. (2014) 'Optimization of running strategies based on anaerobic energy and variations of velocity', *SIAM Journal on Applied Mathematics*, Vol. 74, No. 5, pp.1615–1636.

Altini, M., Penders, J. and Amft, O. (2015) 'Estimating oxygen uptake during nonsteady-state activities and transitions using wearable sensors', *IEEE Journal of Biomedical and Health Informatics*, Vol. 20, No. 2, pp.469–475.

Atkinson, G., Davison, R., Jeukendrup, A. and Passfield, L. (2003) 'Science and cycling: current knowledge and future directions for research', *Journal of Sports Sciences*, Vol. 21, No. 9, pp.767–787.

Barstow, T.J. and Molé, P.A. (1991) 'Linear and nonlinear characteristics of oxygen uptake kinetics during heavy exercise', *Journal of Applied Physiology*, Vol. 71, No. 6, pp.2099–2106.

Beaver, W.L., Wasserman, K. and Whipp, B.J. (1986) 'A new method for detecting anaerobic threshold by gas exchange', *Journal of Applied Physiology*, Vol. 60, No. 6, pp.2020–2027.

Bell, C., Paterson, D.H., Kowalchuk, J.M., Padilla, J. and Cunningham, D.A. (2001) 'A comparison of modelling techniques used to characterise oxygen uptake kinetics during the on-transient of exercise', *Experimental Physiology*, Vol. 86, No. 5, pp.667–676.

Beltrame, T., Amelard, R., Wong, A. and Hughson, R.L. (2017) 'Prediction of oxygen uptake dynamics by machine learning analysis of wearable sensors during activities of daily living', *Scientific Reports*, Vol. 7, No. 1, pp.1–8.

Box, G.E., Jenkins, G.M., Reinsel, G.C. and Ljung, G.M. (2015) *Time Series Analysis: Forecasting and Control*, John Wiley & Sons, Hoboken, New Jersey.

Casaburi, R., Barstow, T.J., Robinson, T. and Wasserman, K. (1989) 'Influence of work rate on ventilatory and gas exchange kinetics', *Journal of Applied Physiology*, Vol. 67, No. 2, pp.547–555.

Gaskill, S.E., Ruby, B.C., Walker, A.J., Sanchez, O.A., Serfass, R.C. and Leon, A.S. (2001) 'Validity and reliability of combining three methods to determine ventilatory threshold', *Medicine & Science in Sports & Exercise*, Vol. 33, No. 11, pp.1841–1848.

Hill, A. and Lupton, H. (1923) 'Muscular exercise, lactic acid, and the supply and utilization of oxygen', *QJM: An International Journal of Medicine*, Vol. 16, No. 62, pp.135–171.

Huang, J. and Zhao, J. (2018) 'Identification of multi-model LPV model with two scheduling variables using transition test', *International Journal of Modelling, Identification and Control*, Vol. 29, No. 1, pp.31–43.

Hughson, R.L., Sherrill, D.L. and Swanson, G.D. (1988) 'Kinetics of VO2 with impulse and step exercise in humans', *Journal of Applied Physiology*, Vol. 64, No. 1, pp.451–459.

Issekutz Jr., B. and Rodahl, K. (1961) 'Respiratory quotient during exercise', *Journal of Applied Physiology*, Vol. 16, No. 4, pp.606–610.

Krogh, A. and Lindhard, J. (1913) 'The regulation of respiration and circulation during the initial stages of muscular work', *The Journal of Physiology*, Vol. 47, Nos. 1–2, pp.112–136.

Le, A., Jaitner, T., Tobias, F. and Litz, L. (2008) 'A dynamic heart rate prediction model for training optimization in cycling', *Proceedings of 7th ISEA Conference 2008*, Engineering of Sport, Springer, Biarritz, 2–6 June, Vol. 7, pp.425–433.

McArdle, W.D., Katch, F.I. and Katch, V.L. (2006) *Essentials of Exercise Physiology*, Lippincott Williams & Wilkins, Baltimore, MD.

Meyer, D. and Senner, V. (2018) 'Evaluating a heart rate regulation system for human-electric hybrid vehicles', *Proceedings of the Institution of Mechanical Engineers, Part P: Journal of Sports Engineering and Technology*, Vol. 232, No. 2, pp.102–111.

Morton, R.H. (2006) 'The critical power and related whole-body bioenergetic models', *European Journal of Applied Physiology*, Vol. 96, No. 4, pp.339–354.

Noakes, T. (2000) 'Physiological models to understand exercise fatigue and the adaptations that predict or enhance athletic performance', *Scandinavian Journal of Medicine & Science in Sports*, Vol. 10, No. 3, pp.123–145.

Olds, T.S., Norton, K. and Craig, N. (1993) 'Mathematical model of cycling performance', *Journal of Applied Physiology*, Vol. 75, No. 2, pp.730–737.

Péronnet, F. and Aguilaniu, B. (2006) 'Lactic acid buffering, nonmetabolic CO_2 and exercise hyperventilation: a critical reappraisal', *Respiratory Physiology & Neurobiology*, Vol. 150, No. 1, pp.4–18.

Pal, T., Dutta, P.K. and Maka, S. (2020) 'Oxygen therapy in chronic obstructive pulmonary disease: insight from convex optimisation', *International Journal of Modelling, Identification and Control*, Vol. 34, No. 2, pp.137–146.

Rosero, N., Martinez, J.J. and Corno, M. (2018) 'Modeling of gas exchange dynamics using cycle-ergometer tests', in *9th Vienna International Conference on Mathematical Modelling*, Vol. 51, pp.349–354.

Rosero, N., Martinez, J.J., Chorin, M. and Vergès, S. (2021) 'Estimation of carbon-dioxide production during cycling by using a set-membership observer', in *2021 European Control Conference (ECC)*, IEEE, pp.2323–2328.

Savkin, A.V., Celler, B.G. et al. (2012) 'Estimation of oxygen consumption during cycling and rowing', in *2012 Annual International Conference of the IEEE Engineering in Medicine and Biology Society*, IEEE, pp.711–714.

Sename, O., Gaspar, P. and Bokor, J. (2013) *Robust Control and Linear Parameter Varying Approaches: Application to Vehicle Dynamics, LNCIS*, Spinger, No. 437.

Shandhi, M.M.H., Bartlett, W.H., Heller, J., Etemadi, M., Young, A., Ploetz, T. and Inan, O. (2020) 'Estimation of instantaneous oxygen uptake during exercise and daily activities using a wearable cardio-electromechanical and environmental sensor', *IEEE Journal of Biomedical and Health Informatics*, Vol. 25, No. 3, pp.634–646.

Solberg, G., Robstad, B., Skjønsberg, O.H. and Borchsenius, F. (2005) 'Respiratory gas exchange indices for estimating the anaerobic threshold', *Journal of Sports Science & Medicine*, Vol. 4, No. 1, p.29, Department of Sports Medicine, Medical Faculty of Uludag University.

Su, S.W., Wang, L., Celler, B.G. and Savkin, A.V. (2007) 'Oxygen uptake estimation in humans during exercise using a hammerstein model', *Annals of Biomedical Engineering*, Vol. 35, No. 11, pp.1898–1906.

Wasserman, K., Whipp, B.J., Koyl, S. and Beaver, W. (1973) 'Anaerobic threshold and respiratory gas exchange during exercise', *Journal of Applied Physiology*, Vol. 35, No. 2, pp.236–243.

Wasserman, K., Hansen, J.E., Sue, D.Y., Stringer, W.W. and Whipp, B.J. (2005) 'Principles of exercise testing and interpretation: including pathophysiology and clinical applications', *Medicine & Science in Sports & Exercise*, Vol. 37, No. 7, p.1249.